Supporting information for

A Synthetic Single-Site Fe Nitrogenase: High Turnover, Freeze-Quench ^{57}Fe Mössbauer Data, and a Hydride Resting State

Trevor J. Del Castillo[†], Niklas B. Thompson[†], and Jonas C. Peters

[†]T.J.D.C. and N.B.T. contributed equally to this work.

Division of Chemistry and Chemical Engineering, California Institute of Technology, Pasadena, California 91125, United States

Table of Contents:

S1–3	Experimental and synthetic details
S3–6	Ammonia production and quantification studies
S7	Ammonia generation reaction with periodic substrate reloading
S8–12	Time-resolved NH_3 quantification via low-temperature quenching
S13	Time-resolved H_2 quantification studies
S14	Solution IR calibration of [Na(12-crown-4)$_2$][P_3^BFe-N_2] (**1**)
S15–17	Stoichiometric reaction of (P_3^B)(μ-H)Fe(H)(N_2) (**4-N_2**) with $HBAr^F_4$ and KC_8
S18–28	Mössbauer Spectra
S29	Controlled Potential Electrolysis of [P_3^BFe][BAr^F_4] and 10 equiv $HBAr^F_4$
S29	References

1. Experimental details

1.1 General considerations:

All manipulations were carried out using standard Schlenk or glovebox techniques under an N_2 atmosphere. Solvents were deoxygenated and dried by thoroughly sparging with N_2 followed by passage through an activated alumina column in a solvent purification system by SG Water, USA LLC. Nonhalogenated solvents were tested with sodium benzophenone ketyl in tetrahydrofuran (THF) in order to confirm the absence of oxygen and water. Deuterated solvents were purchased from Cambridge Isotope Laboratories, Inc., degassed, and dried over activated 3-Å molecular sieves prior to use.

KC_8,[1] [Na(12-crown-4)$_2$][P_3^BFe-N_2] (**1**),[2] [K(OEt_2)$_{0.5}$][P_3^CFe-N_2] (**2**),[3] [Na(12-crown-4)$_2$][P_3^{Si}Fe-N_2] (**3**),[4] (P_3^B)(μ-H)Fe(H)(N_2) (**4-N_2**),[5] (P_3^B)(μ-H)Fe(H)(N_2) (**4-H_2**),[5] [P_3^BFe-NH_3][BAr^F_4],[6] [P_3^BFe-

$N_2H_4][BAr^F_4]$,[6] $P_3^BFe\text{-}NH_2$,[6] $[P_3^BFe][BAr^F_4]$,[6] $P_3^BFe\text{-}NAd$,[7] and $[P_3^BFe\text{-}NAd][BAr^F_4]$[7] were prepared according to literature procedures. $NaBAr^F_4$ and $[H(OEt_2)_2][BAr^F_4]$ ($HBAr^F_4$) were prepared and purified according to a procedure modified from the literature as described below. All other reagents were purchased from commercial vendors and used without further purification unless otherwise stated. Diethyl ether (Et_2O) and THF used NH_3 generation experiments were stirred over Na/K (≥ 2 hours) and filtered before use.

1.2 Physical Methods:

^1H chemical shifts are reported in ppm relative to tetramethylsilane, using ^1H resonances from residual solvent as internal standards. IR measurements were obtained as solutions or thin films formed by evaporation of solutions using a Bruker Alpha Platinum ATR spectrometer with OPUS software (solution IR collected in a cell with KBr windows and a 1 mm pathlength). Optical spectroscopy measurements were collected with a Cary 50 UV-vis spectrophotometer using a 1-cm two-window quartz cell. H_2 was quantified on an Agilent 7890A gas chromatograph (HP-PLOT U, 30 m, 0.32 mm ID; 30 °C isothermal; nitrogen carrier gas) using a thermal conductivity detector. Cyclic voltammetry measurements were carried out in a glovebox under an N_2 atmosphere in a one-compartment cell using a CH Instruments 600B electrochemical analyzer. A glassy carbon electrode was used as the working electrode and platinum wire was used as the auxiliary electrode. The reference electrode was Ag/AgOTf in Et_2O isolated by a CoralPor™ frit (obtained from BASi). The ferrocene couple (Fc/Fc^+) was used as an external reference. Et_2O solutions of electrolyte (0.1 M $NaBAr^F_4$) and analyte were also prepared under an inert atmosphere.

1.3 Mössbauer Spectroscopy:

Mössbauer spectra were recorded on a spectrometer from SEE Co. (Edina, MN) operating in the constant acceleration mode in a transmission geometry. The sample was kept in an SVT-400 cryostat form Janis (Wilmington, MA). The quoted isomer shifts are relative to the centroid of the spectrum of a metallic foil of α-Fe at room temperature. Solid samples were prepared by grinding solid material into a fine powder and then mounted in to a Delrin cup fitted with a screw-cap as a boron nitride pellet. Solution samples were transferred to a sample cup and chilled to 77 K inside of the glovebox, and unless noted otherwise, quickly removed from the glovebox and immersed in liquid N_2 until mounted in the cryostat. Data analysis was performed using version 4 of the program WMOSS (www.wmoss.org) and quadrupole doublets were fit to Lorentzian lineshapes. See discussion below for detailed notes on the fitting procedure.

1.4 Ammonia Quantification:

Reaction mixtures are cooled to 77 K and allowed to freeze. The reaction vessel is then opened to atmosphere and to the frozen solution is slowly added a fourfold excess (with respect to acid) solution of a NaO^tBu solution in MeOH (0.25 mM) over 1–2 minutes. This solution is allowed to freeze, then the headspace of the tube is evacuated and the tube is sealed. The tube is then allowed to warm to RT and stirred at room temperature for 10 minutes. An additional Schlenk tube is charged with HCl (3 mL of a 2.0 M solution in Et_2O, 6 mmol) to serve as a collection flask. The volatiles of the reaction mixture are vacuum transferred into this collection flask. After completion of the vacuum transfer, the collection flask is sealed and warmed to room temperature. Solvent is removed in vacuo, and the remaining residue is dissolved in H_2O (1 mL). An aliquot of this solution (20–100 μL) is then analyzed for the presence of NH_3 (present as NH_4Cl) by the indophenol method.[8] Quantification is performed with UV−vis spectroscopy by analyzing absorbance at 635 nm.

2. Synthetic Details:

2.1 Synthesis and Purification of $NaBAr^F_4$ and $[H(OEt_2)_2][BAr^F_4]$:

Crude $NaBAr^F_4$ was prepared according to a literature procedure.[9] The crude material, possessing a yellow-tan hue, was purified by a modification to the procedure published by Bergman,[10] as follows. The

crude $NaBAr^F_4$ was ground into a fine powder and partially hydrated by exposure to air for at least 24 hours ($NaBAr^F_4$ is a hygroscopic solid and crystallizes as a hydrate containing between 0.5–3.0 equivalents of H_2O when isolated under air). This material was first washed with dichloromethane (~3 mL/g, in three portions), washing liberally with pentane between each portion of dichloromethane. The remaining solids were washed with boiling fluorobenzene (~1 mL/g, in three portions), to yield a bright white powder. Anhydrous $NaBAr^F_4$ was obtained by drying this material under vacuum at 100 °C over P_2O_5 for at least 18 hours. Note that additional $NaBAr^F_4$ may be recrystallized from the fluorobenzene washings via slow diffusion of pentane vapors at room temperature, and further purified if necessary.

Crude $[H(OEt_2)_2][BAr^F_4]$ was prepared according to a literature procedure, using $NaBAr^F_4$ purified as described above.[11] The crude material was purified by iterative recrystallization from 4 mL/g Et_2O layered with an equivalent volume of pentane at -30 °C. The purity of the recrystallized $[H(OEt_2)_2][BAr^F_4]$ was assayed by collecting a UV-vis spectrum of a 10 mM solution in Et_2O, where the presence of yellow-brown impurities appears as a broad absorbance centered at ~330 nm (see Fig. S2.1). Typically 2–3 recrystallizations were required to obtain material of suitable purity for catalytic reactions.

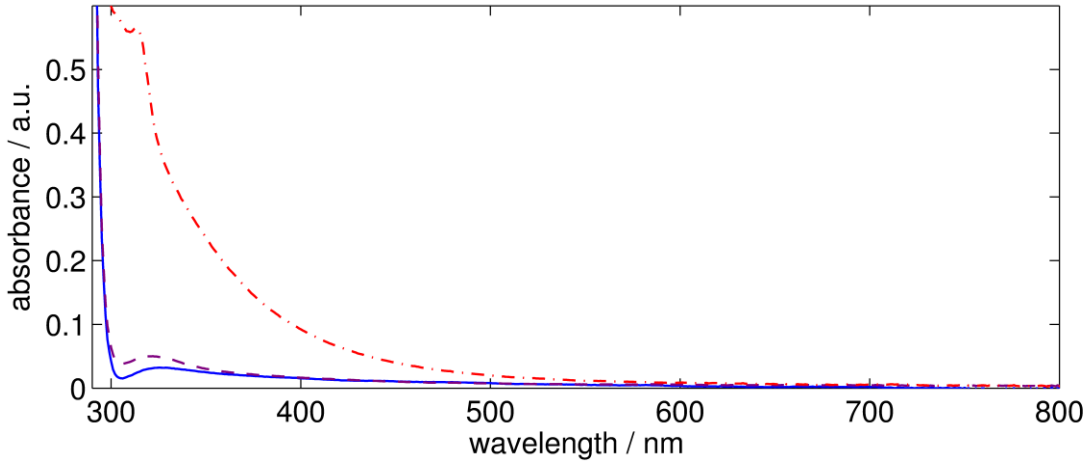

Figure S2.1: UV-vis traces of 10 mM solutions of $[H(OEt_2)_2][BAr^F_4]$ in Et_2O at various stages of purity. (Red dash-dotted trace) $[H(OEt_2)_2][BAr^F_4]$ prepared from crude $NaBAr^F_4$ without additional purification; (Purple dotted trace) $[H(OEt_2)_2][BAr^F_4]$ prepared from $NaBAr^F_4$ purified according to the above procedure, and recrystallized once; (Blue solid trace) $[H(OEt_2)_2][BAr^F_4]$ prepared from $NaBAr^F_4$ purified according to the above procedure, and recrystallized twice.

2.2 Preparation of 10 wt% Na(Hg) shot:

In a three-neck round bottom flask equipped with a mechanical stirrer, reflux condenser, and a dropping funnel was added Na (0.5 g) and a sufficient volume of toluene to completely submerse the Na. The dropping funnel was charged with 5 grams of Hg. The toluene was brought to reflux and the molten Na was finely dispersed by rapid agitation with the mechanical stirrer, at which point the Hg was added in one shot. *Caution: upon contact with Na, the Hg vapors boil and there is a brief but intense exotherm.* The pelleted 10 wt% Na(Hg) immediately forms, at which point the toluene is decanted, and the shot is washed with Et_2O and pentane before being dried in vacuo. After breaking up coagulated pieces, this procedure yields somewhat uniform shot ranging 1–3 mm in diameter.

3. Ammonia production and quantification studies

3.1 Standard NH_3 Generation Reaction Procedure with $[Na(12\text{-crown-}4)_2][P_3{}^BFe\text{-}N_2]$ (1):

All solvents are stirred with Na/K for ≥2 hours and filtered prior to use. In a nitrogen-filled glovebox, a stock solution of **1** in THF (9.5 mM) is prepared. Note that a fresh stock solution is prepared for each experiment and used immediately. An aliquot of this stock solution (50–200 μL, 0.47–1.9 μmol) is added to a Schlenk tube and evaporated to dryness under vacuum, depositing a film of **1**. The tube is then charged with a stir bar and cooled to 77 K in a cold well. To the cold tube is added a solution of $HBAr^F_4$ in Et_2O. This solution is allowed to cool and freeze for 5 minutes. Then a suspension of KC_8 in Et_2O (1.2 equiv relative to $HBAr^F_4$) is added to the cold tube. The temperature of the system is allowed to equilibrate for 5 minutes and then the tube is sealed with a Teflon screw-valve. This tube is passed out of the box into a liquid N_2 bath and transported to a fume hood. The tube is then transferred to a dry ice/acetone bath where it thaws and is allowed to stir at -78 °C for the desired length of time. At this point the tube is allowed to warm to room temperature with stirring, and stirred at room temperature for 5 minutes. To ensure reproducibility, all experiments were conducted in 200 mL Schlenk tubes (51 mm OD) using 25 mm stir bars, and stirring was conducted at ~900 rpm.

Table S3.1: UV-vis quantification results for standard NH_3 generation experiments with **1**

Entry	Total volume of Et_2O (mL)	1 μmol (mM)	$[H(OEt_2)_2][BAr^F_4]$ equiv (mM)	NH_4Cl (μmol)	Equiv NH_3/Fe	% Yield Based on H^+
A	1.5	1.9 (1.3)	48 (63)	13.2	7.0	43.2
B	1.5	1.9 (1.3)	48 (63)	14.5	7.6	47.2
Avg.	—	—	—	—	7.3 ± 0.5	45 ± 3
C	3.0	1.9 (0.64)	97 (63)	22.1	11.6	35.9
D	3.0	1.9 (0.64)	97 (63)	25.1	13.2	40.8
Avg.	—	—	—	—	12 ± 1	38 ± 3
E	1.1	0.48 (0.43)	150 (63)	8.34	17.5	36.1
F	1.1	0.48 (0.43)	150 (63)	8.19	17.2	35.5
Avg.	—	—	—	—	17.4 ± 0.2	35.8 ± 0.4
G	5.5	0.48 (0.087)	730 (63)	23.3	48.9	20.2
H	5.5	0.48 (0.087)	730 (63)	20.3	42.5	17.6
I	5.5	0.48 (0.087)	730 (63)	19.1	40.2	16.6
J	1.4	0.12 (0.087)	730 (63)	4.82	40.5	16.7
Avg.	—	—	—	—	43 ± 4	18 ± 2
K	11.0	0.48 (0.043)	1500 (63)	28.4	59.5	12.3
L	11.0	0.48 (0.043)	1500 (63)	27.1	56.8	11.7
M	11.0	0.48 (0.043)	1500 (63)	22.9	48.1	9.9
N	11.0	0.48 (0.043)	1500 (63)	25.4	53.4	11.0
O	11.0	0.48 (0.043)	1500 (63)	30.2	63.5	13.1
P	2.8	0.12 (0.043)	1500 (63)	7.67	64.4	13.3
Q	2.8	0.12 (0.043)	1500 (63)	7.53	63.3	13.0
R	2.8	0.12 (0.043)	1500 (63)	7.67	64.4	13.3
S	2.8	0.12 (0.043)	1500 (63)	6.85	57.5	11.9
Avg.	—	—	—	—	59 ± 6	12 ± 1

Hydrazine was not detected in the catalytic runs using a standard UV-Vis quantification method.[12]

3.2 Standard NH_3 Generation Reaction Procedure with $[K(OEt_2)_{0.5}][P_3^CFe\text{-}N_2]$ (2):

The procedure was identical to that of the standard NH_3 generation reaction protocol with the changes noted. The precursor used was **2**.

Table S3.2: UV-vis quantification results for standard NH_3 generation experiments with **2**

Entry	Total volume of Et_2O (mL)	2 µmol (mM)	$[H(OEt_2)_2][BAr^F_4]$ equiv (mM)	NH_4Cl (µmol)	Equiv NH_3/Fe	% Yield Based on H^+
A*	2.5	2.5 (1.0)	37 (37)	—	4.6 ± 0.8	36 ± 6
B	1.1	0.63 (0.56)	110 (60)	6.66	10.7	29.7
C	1.1	0.63 (0.56)	110 (60)	7.41	11.9	33.0
Avg.	—	—	—	—	11.3 ± 0.9	31 ± 2
D	2.3	0.63 (0.28)	220 (60)	7.41	11.9	16.4
E	2.3	0.63 (0.28)	220 (60)	9.89	15.8	21.9
Avg.	—	—	—	—	14 ± 3	19 ± 4
F	2.0	0.16 (0.080)	750 (60)	2.49	15.6	6.2
G	2.0	0.16 (0.080)	750 (60)	3.50	21.9	8.8
Avg.	—	—	—	—	19 ± 4	7 ± 2
H	4.0	0.16 (0.040)	1500 (60)	7.46	46.8	9.3
I	4.0	0.16 (0.040)	1500 (60)	4.63	29.0	5.8
J	4.0	0.16 (0.040)	1500 (60)	5.82	36.5	7.3
K	4.0	0.16 (0.040)	1500 (60)	5.56	34.8	6.9
L	4.0	0.16 (0.040)	1500 (60)	5.13	32.1	6.4
Avg.	—	—	—	—	36 ± 7	7 ± 1

Hydrazine was not detected in the catalytic runs using a standard UV-Vis quantification method.[12]
* Data for entry A is an average of experiments described in reference 3.

3.3 Standard NH_3 Generation Reaction Procedure with $[Na(12\text{-crown-}4)_2][P_3^{Si}Fe\text{-}N_2]$ (3):

The procedure was identical to that of the standard NH_3 generation reaction protocol with the changes noted. The precursor used was **3**.

Table S3.3: UV-vis quantification results for standard NH_3 generation experiments with **3**

Entry	Total volume of Et_2O (mL)	3 µmol (mM)	$[H(OEt_2)_2][BAr^F_4]$ equiv (mM)	NH_4Cl (µmol)	Equiv NH_3/Fe	% Yield Based on H^+
A*	3.25	1.9 (0.58)	49 (28)	—	0.8 ± 0.5	5 ± 3
B	3.0	0.12 (0.039)	1500 (60)	0.516	4.4	0.9
C	3.0	0.12 (0.039)	1500 (60)	0.380	3.2	0.6
Avg.	—	—	—	—	3.8 ± 0.8	0.8 ± 0.2

Hydrazine was not detected in the catalytic runs using a standard UV-Vis quantification method.[12]
* Data for entry A is an average of experiments described in reference 13.

3.4 Standard NH_3 Generation Reaction Procedure with $(P_3^B)(\mu\text{-}H)Fe(H)(N_2)$ (4-N_2):

The procedure was identical to that of the standard NH_3 generation reaction protocol with the changes noted. The precursor used was **4-N2**. Note that **4-N_2** is not indefinitely stable in the solid state, even at -30 °C; accordingly **4-N_2** was used within 24 hours after isolation as a solid. The addition of toluene was necessary to load the precatalyst volumetrically. The final solvent composition for entries A and B was 3% toluene in Et_2O. The final solvent composition for entries C and D was 25% toluene in Et_2O.

Table S3.4: UV-vis quantification results for standard NH_3 generation experiments with **4-N_2**

Entry	Total volume of (mL)	4-N_2 µmol (mM)	$[H(OEt_2)_2][BAr^F_4]$ equiv (mM)	NH_4Cl (µmol)	Equiv NH_3/Fe	% Yield Based on H^+
A	1.1	0.48 (*)	150 (63)	0.582	1.19	2.56
B	1.1	0.48 (*)	150 (63)	0.490	1.00	2.15
Avg.	—	—	—	—	1.1 ± 0.1	2.4 ± 0.3
C	1.7	0.74 (0.44)	150 (63)	3.66	4.95	10.3
D	1.7	0.74 (0.44)	150 (63)	4.63	6.26	13.0
Avg.	—	—	—	—	5.6 ± 0.9	12 ± 2

Hydrazine was not detected in the catalytic runs using a standard UV-Vis quantification method.[12]
* **4-N_2** not fully soluble under these conditions.

3.5 NH_3 Generation Reaction Procedure with (1) with the inclusion of NH_3:

A standard catalytic reaction was prepared according to the procedure detailed in section 3.1. After the frozen Schlenk tube was removed from the glovebox, it was brought to a Schlenk line and attached to the line via a 0.31 mL calibrated volume (corresponding to 12.7 µmol gas when filled at 21 °C and 1 atm). The gas manifold of the line was first filled with N_2 by three pump-refill cycles, and subsequently sparged (through a mineral oil bubbler) with $NH_{3(g)}$ for 30 minutes, passing the $NH_{3(g)}$ through a -30 °C trap to remove adventitious water. At this point the calibrated volume was filled with $NH_{3(g)}$ via 5 pump-refill cycles, and then sealed from the gas manifold. The frozen Schlenk tube was opened and allowed to equilibrate with the calibrated volume for 1 hour before it was resealed, and the reaction carried out in the usual manner. As a control, several trials were conducted with only an 2.0 M ethereal solution of HCl frozen in the tube, and it assumed that the average amount of NH_3 recovered in those trials was added to the catalytic reactions.

Table S3.5: UV-vis quantification results for NH_3 generation experiments with **1** with the inclusion of NH_3

Entry	Total volume of Et_2O (mL)	1 µmol (mM)	$[H(OEt_2)_2][BAr^F_4]$ equiv (mM)	NH_4Cl (µmol)	NH_4Cl due to Fe (µmol)	Equiv NH_3/Fe
A	3.0	0	0	12.5	N/A	N/A
B	3.0	0	0	11.8	N/A	N/A
C	3.0	0	0	12.1	N/A	N/A
D	3.0	0	0	12.0	N/A	N/A
E	3.0	0	0	12.2	N/A	N/A
Avg.	—	—	—	12.1 (95 % of expected value)		
C	1.1	0.48 (0.43)	150 (63)	15.1	3.0	6.3
D	1.1	0.48 (0.43)	150 (63)	15.2	3.1	6.5
Avg.	—	—	—	—	—	6.4 ± 0.1

Hydrazine was not detected in the catalytic runs using a standard UV-Vis quantification method.[12]

3.6 Standard NH_3 Generation Reaction Procedure with 1 using Na(Hg) as the reductant:

The procedure was identical to that of the standard NH_3 generation reaction protocol with the changes noted. The precursor used was **1** and 10 wt% Na(Hg) shot of approximately 1–3 mm diameter was employed as the reductant (1900 Na atom equiv relative to catalyst).

Table S3.6: UV-vis quantification results for standard NH_3 generation experiments with **1** using Na(Hg) as the reductant

Entry	Total volume of Et_2O (mL)	1 µmol (mM)	$[H(OEt_2)_2][BAr^F_4]$ equiv (mM)	NH_4Cl (µmol)	Equiv NH_3/Fe	% Yield Based on H^+
A	1.1	0.48 (0.43)	150 (63)	2.45	5.15	10.6
B	1.1	0.48 (0.43)	150 (63)	2.30	4.84	9.97
Avg.	—	—	—	—	5.0 ± 0.2	10.3 ± 0.5

Hydrazine was not detected in the catalytic runs using a standard UV-Vis quantification method.[12]

4. NH_3 Generation Reaction with Periodic Substrate Reloading, Procedure with 1:

All solvents are stirred with Na/K for ≥2 hours and filtered prior to use. In a nitrogen-filled glovebox, a stock solution of $[Na(12\text{-crown-}4)_2][P_3^BFe\text{-}N_2]$ (**1**) in THF (9.5 mM) is prepared. Note that a fresh stock solution is prepared for each experiment and used immediately. An aliquot of this stock solution (50-200 µL, 0.47-1.9 µmol) is added to a Schlenk tube. This aliquot is evaporated to dryness under vacuum, depositing a film of **1**. The tube is then charged with a stir bar and cooled to 77 K in a cold well. To the cold tube is added a solution of $HBAr^F_4$ (48 equiv with respect to **1**) in Et_2O. This solution is allowed to cool and freeze for 5 minutes. Then a suspension of KC_8 (1.3 equiv with respect to $HBAr^F_4$) in Et_2O is added to the cold tube. The temperature of the system is allowed to equilibrate for 5 minutes and then the tube is sealed. The cold well cooling bath is switched from a $N_{2(l)}$ bath to a dry ice/acetone bath. In the cold well the mixture in the sealed tube thaws with stirring and is allowed to stir at -78 °C for 40 minutes. Then, without allowing the tube to warm above -78 °C, the cold well bath is switched from dry ice/acetone to $N_{2(l)}$. After ten minutes the reaction mixture is observed to have frozen, at this time the tube is opened. To the cold tube is added a solution of $HBAr^F_4$ (48 equiv with respect to **1**) in Et_2O. This solution is allowed to cool and freeze for 5 minutes. Then a suspension of KC_8 (1.3 equiv with respect to $HBAr^F_4$) in Et_2O is added to the cold tube. The temperature of the system is allowed to equilibrate for 5 minutes and then the tube is sealed. The cold well cooling bath is switched from a $N_{2(l)}$ bath to a dry ice/acetone bath. In the cold well the mixture in the sealed tube thaws with stirring and is allowed to stir at -78 °C for 40 minutes. These last steps are repeated for the desired number of loadings. Then the tube is allowed to warm to RT with stirring, and stirred at RT for 5 minutes.

Table S4.1: UV-vis quantification results for NH_3 generation experiments with 1, with reloading

Entry	Number of Loadings	4-N_2 µmol	$[H(OEt_2)_2][BAr^F_4]$ equiv	NH_4Cl (µmol)	Equiv NH_3/Fe	% Yield Based on H^+
A	1	1.9	48	13.3	6.96	43.2
B	1	1.9	48	14.5	7.60	47.2
Avg.	—	—	—	—	7.3 ± 0.5	45 ± 3
C	2	0.95	96	9.56	10.0	31.5
D	2	0.95	96	10.3	10.9	34.0
Avg.	—	—	—	—	10.4 ± 0.6	33 ± 2
C	2	0.95	150	13.4	14.1	32.7
D	2	0.95	150	14.9	15.6	29.4
Avg.	—	—	—	—	15 ± 1	31 ± 2
C	2	1.0	190	18.4	17.6	29.0
D	2	1.0	190	18.4	17.6	29.0
Avg.	—	—	—	—	17.6	29

5. General Procedure for Time-resolved NH_3 Quantification via Low-temperature Quenching:

A typical catalytic reaction is prepared according to the procedure described above. The timer is set to zero as soon as the frozen reaction mixture is transferred to the dry ice/acetone bath; note that the average thaw time is 2.0 ± 0.3 minutes (measured for a 1.1 mL solution of Et_2O over 8 trials). At the desired reaction time, the Schlenk tube is rapidly transferred to a liquid N_2 bath and the reaction mixture is allowed to freeze. Under N_2 counterflow, a solution of ^{t}BuLi (1.6 M in hexanes, 4 equiv with respect to $HBAr^F_4$ is added to the frozen reaction mixture. The Schlenk tube is then sealed, thawed to -78 °C, and stirred rapidly for 10 minutes. The Schlenk tube is transferred to a liquid N_2 bath and the reaction mixture is re-frozen. The reaction vessel is opened to atmosphere and to the frozen solution is slowly added a fivefold excess (with respect to $HBAr^F_4$) solution of a NaO^tBu solution in MeOH (0.25 mM) over 1–2 minutes. This solution is allowed to freeze, then the headspace of the tube is evacuated and the tube is sealed. The tube is then allowed to warm to RT and stirred at room temperature for 10 minutes. At this point the reaction is quantified for the presence of NH_3 (*vide supra*).

As a control to determine that the action of ^{t}BuLi is sufficiently fast to enable rapid quenching of catalytic reactions at low temperature, we added ^{t}BuLi to reaction mixtures prepared as described above before allowing them to thaw to -78 °C for the first time (effectively at time 0, Table S5.1, Entry A) and observed no detectable NH_3 formation.

Table S5.1: Time profiles for NH_3 generation by **1**

Entry	Total volume of Et_2O (mL)	1 µmol (mM)	$[H(OEt_2)_2][BAr^F_4]$ equiv (mM)	Quench time (min)	$[NH_3]$ (mM)	Equiv NH_3/Fe
A	3.0	1.9 (0.64)	48 (31)	0	0	0
B	3.0	1.9 (0.64)	48 (31)	5	1.21	1.91
C	3.0	1.9 (0.64)	48 (31)	5	1.87	2.94
Avg.	—	—	—	5	1.5 ± 0.5	2.4 ± 0.2
D	3.0	1.9 (0.64)	48 (31)	10	4.36	6.86
E	3.0	1.9 (0.64)	48 (31)	10	3.66	5.76
Avg.	—	—	—	10	4.0 ± 0.5	6.3 ± 0.8
F	3.0	1.9 (0.64)	48 (31)	15	4.87	7.68
G	3.0	1.9 (0.64)	48 (31)	15	4.63	7.29
Avg.	—	—	—	15	4.8 ± 0.2	7.5 ± 0.3
H	3.0	1.9 (0.64)	48 (31)	25	4.40	6.93
I	3.0	1.9 (0.64)	48 (31)	25	4.79	7.54
Avg.	—	—	—	25	4.6 ± 0.3	7.2 ± 0.4
J	1.1	0.48 (0.43)	150 (63)	5	0.806	1.86
K	1.1	0.48 (0.43)	150 (63)	5	1.09	2.51
Avg.	—	—	—	5	0.9 ± 0.2	2.2 ± 0.5
L	1.1	0.48 (0.43)	150 (63)	10	2.08	4.81
M	1.1	0.48 (0.43)	150 (63)	10	2.74	6.33
Avg.	—	—	—	10	2.4 ± 0.5	6 ± 1
N	1.1	0.48 (0.43)	150 (63)	15	3.79	8.75
O	1.1	0.48 (0.43)	150 (63)	15	4.06	9.39
Avg.	—	—	—	15	3.9 ± 0.2	9.1 ± 0.4
P	1.1	0.48 (0.43)	150 (63)	25	5.73	13.2
Q	1.1	0.48 (0.43)	150 (63)	25	4.68	10.8
Avg.	—	—	—	25	5.2 ± 0.7	12 ± 2
R	1.1	0.48 (0.43)	150 (63)	35	6.11	14.1

S	1.1	0.48 (0.43)	150 (63)	35	5.51	12.7
Avg.	—	—	—	35	5.8 ± 0.4	13 ± 1
T	1.1	0.48 (0.43)	150 (63)	45	7.99	18.5
U	1.1	0.48 (0.43)	150 (63)	45	8.37	19.3
Avg.	—	—	—	45	8.2 ± 0.3	18.9 ± 0.6
V	1.1	0.48 (0.43)	150 (63)	55	7.18	16.6
W	1.1	0.48 (0.43)	150 (63)	55	7.94	18.3
Avg.	—	—	—	55	7.6 ± 0.5	17 ± 1

Hydrazine was not detected in the catalytic runs using a standard UV-Vis quantification method.[10]

5.1 Kinetic Study of NH_3 Generation by 1 via the Method of Initial Rates:

General procedure: Typical catalytic reactions were prepared at various concentrations of **1** and $HBAr^F_4$ (1.1 mL Et_2O total for each reaction). For each given concentration of **1** and $HBAr^F_4$, the time profile of NH_3 generation was measured over the first 15 minutes by quenching reactions at 5, 10 and 15 minutes, as described above. The results of individual experiments are given in Table S5.2. The initial rate of NH_3 formation, $v_0 = \frac{d[NH_3]}{dt}(0)$ was measured as the slope of a least-squares linear regression for these data. For the cases where the timescale of the reaction was too fast to obtain pseudo-first-order behavior over the first 15 minutes, v_0 was approximated as the slope of the line between the yield of NH_3 at 5 minutes and a zero point at 2 minutes (the average thaw time for the reaction, *vide supra*); the results of this analysis are given in Table S5.3 and plotted in Figures S5.1 and S5.2. The reaction order in **1** and $HBAr^F_4$ was determined by applying a least-squares linear analysis to the initial rates determined for 5 different concentrations in each reagent, ranging over a factor of 16 (Table S5.4).

Table S5.2: Time resolved NH_3 quantification data used in initial rates analysis for NH_3 generation by **1**

Entry	**Total volume of Et_2O (mL)**	**1 µmol (mM)**	**$[H(OEt_2)_2][BAr^F_4]$ equiv (mM)**	**Quench time (min)**	**$[NH_3]$ (mM)**
A	1.1	0.12 (0.11)	560 (63)	5	0.268
B	1.1	0.12 (0.11)	560 (63)	5	0.273
Avg.	—	—	—	5	0.270 ± 0.004
C	1.1	0.12 (0.11)	560 (63)	10	0.225
D	1.1	0.12 (0.11)	560 (63)	10	0.338
Avg.	—	—	—	10	0.28 ± 0.08
E	1.1	0.12 (0.11)	560 (63)	15	0.747
F	1.1	0.12 (0.11)	560 (63)	15	1.27
Avg.	—	—	—	15	1.0 ± 0.4
G	1.1	0.24 (0.22)	290 (63)	5	0.538
H	1.1	0.24 (0.22)	290 (63)	5	0.763
Avg.	—	—	—	5	0.7 ± 0.2
I	1.1	0.24 (0.22)	290 (63)	10	1.81
J	1.1	0.24 (0.22)	290 (63)	10	1.29
Avg.	—	—	—	10	1.5 ± 0.4
K	1.1	0.24 (0.22)	290 (63)	15	3.47
L	1.1	0.24 (0.22)	290 (63)	15	2.23
Avg.	—	—	—	15	2.9 ± 0.9
M	1.1	0.95 (0.87)	73 (63)	5	1.98
N	1.1	0.95 (0.87)	73 (63)	5	1.64

Avg.	—	—	—	5	1.8 ± 0.2
O	1.1	0.95 (0.87)	73 (63)	10	5.36
P	1.1	0.95 (0.87)	73 (63)	10	4.20
Avg.	—	—	—	10	4.8 ± 0.8
Q	1.1	0.95 (0.87)	73 (63)	15	9.27
R	1.1	0.95 (0.87)	73 (63)	15	8.84
Avg.	—	—	—	15	9.1 ± 0.3
S	1.1	1.9 (1.7)	36 (63)	5	4.53
T	1.1	1.9 (1.7)	36 (63)	5	7.24
Avg.	—	—	—	5	6 ± 2
U	1.1	1.9 (1.7)	36 (63)	10	10.8
V	1.1	1.9 (1.7)	36 (63)	10	10.3
Avg.	—	—	—	10	10.5 ± 0.3
W	1.1	1.9 (1.7)	36 (63)	15	10.4
X	1.1	1.9 (1.7)	36 (63)	15	10.4
Avg.	—	—	—	15	10.44 ± 0.02
Y	1.1	0.48 (0.43)	35 (15)	5	1.06
Z	1.1	0.48 (0.43)	35 (15)	5	1.27
Avg.	—	—	—	5	1.2 ± 0.2
AA	1.1	0.48 (0.43)	35 (15)	10	1.33
BB	1.1	0.48 (0.43)	35 (15)	10	1.43
Avg.	—	—	—	10	1.38 ± 0.07
CC	1.1	0.48 (0.43)	35 (15)	15	1.26
DD	1.1	0.48 (0.43)	35 (15)	15	1.53
Avg.	—	—	—	15	1.4 ± 0.2
EE	1.1	0.48 (0.43)	68 (30)	5	1.23
FF	1.1	0.48 (0.43)	68 (30)	5	1.29
Avg.	—	—	—	5	1.26 ± 0.04
GG	1.1	0.48 (0.43)	68 (30)	10	3.22
HH	1.1	0.48 (0.43)	68 (30)	10	2.76
Avg.	—	—	—	10	3.0 ± 0.3
II	1.1	0.48 (0.43)	68 (30)	15	3.42
JJ	1.1	0.48 (0.43)	68 (30)	15	3.50
Avg.	—	—	—	15	3.46 ± 0.05
KK	1.1	0.48 (0.43)	290 (130)	5	0.736
LL	1.1	0.48 (0.43)	290 (130)	5	1.04
Avg.	—	—	—	5	0.9 ± 0.2
MM	1.1	0.48 (0.43)	290 (130)	10	4.11
NN	1.1	0.48 (0.43)	290 (130)	10	3.47
Avg.	—	—	—	10	3.8 ± 0.4
OO	1.1	0.48 (0.43)	290 (130)	15	6.24
PP	1.1	0.48 (0.43)	290 (130)	15	6.64
Avg.	—	—	—	15	6.4 ± 0.3
QQ	1.1	0.48 (0.43)	580 (250)	5	0.495
RR	1.1	0.48 (0.43)	580 (250)	5	1.13
Avg.	—	—	—	5	0.8 ± 0.5
SS	1.1	0.48 (0.43)	580 (250)	10	3.56
TT	1.1	0.48 (0.43)	580 (250)	10	2.50

Avg.	—	—	—	10	3.0 ± 0.8
UU	1.1	0.48 (0.43)	580 (250)	15	7.13
VV	1.1	0.48 (0.43)	580 (250)	15	7.40
Avg.	—	—	—	15	7.3 ± 0.2

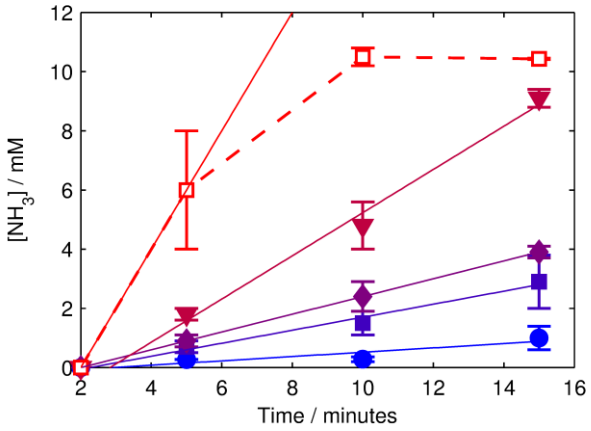

Figure S5.1: Time courses for NH_3 generation by **1** at varying concentrations of **1**. All reactions conducted in 63 mM $HBAr^F_4$ with 1.2 equiv KC_8 with respect to $HBAr^F_4$. (Blue circles) [**1**] = 0.11 mM; (Indigo squares) [**1**] = 0.22 mM; (purple diamonds) [**1**] = 0.43 mM; (maroon triangles) [**1**] = 0.87 mM; (red squares) [**1**] = 1.7 mM. Solid lines show the least-squares linear regression fit to the 5, 10 and 15 minute data, except for the [**1**] = 1.7 mM trace (red squares), which deviates from pseudo-first-order behavior; in this case, the line is fit from the data at 5 minutes to a zero point at t = 2 minutes.

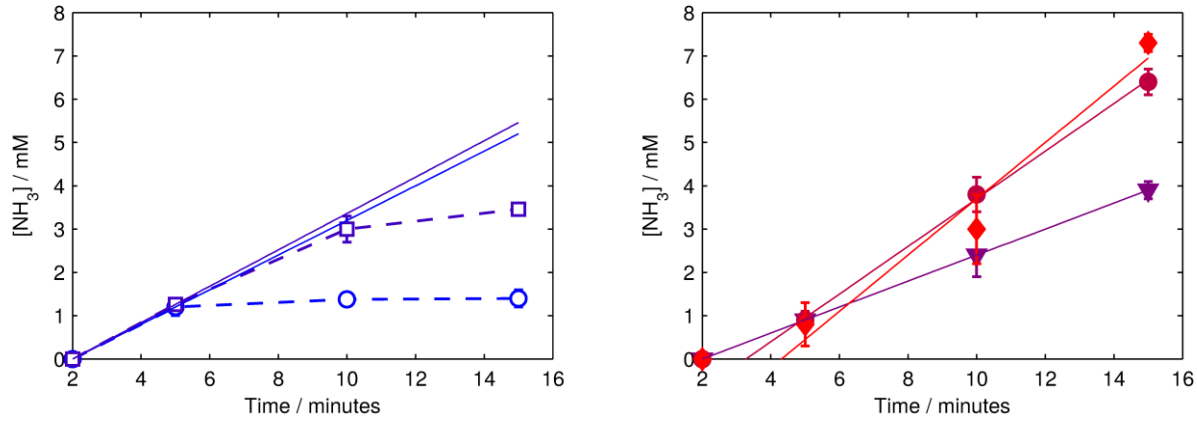

Figure S5.2: Time courses for NH_3 generation by **1** at varying concentrations of $HBAr^F_4$. All reactions conducted in 0.43 mM **1** with 185 equiv KC_8 with respect to **1**. Left: (Blue circles) [$HBAr^F_4$] = 15 mM; (Indigo squares) [$HBAr^F_4$] = 30 mM. Right: (purple triangles) [$HBAr^F_4$] = 63 mM; (maroon circles) [$HBAr^F_4$] = 130 mM; (red diamonds) [$HBAr^F_4$] = 250 mM. Left: Solid lines show the line connecting the 5 minute data with a zero point at t = 2 minutes. Right: solid lines show the least-squares linear regression fit to the 5, 10 and 15 minute data.

Table S5.3: Results of initial rates determination for NH_3 generation **1**

Entry	$[\mathbf{1}]_0$ (mM)	$[[H(OEt_2)_2][BAr^F{}_4]]_0$ (mM)	v_0 (mM min^{-1})	r^2*
A	0.11	63	0.07 ± 0.04	0.76
B	0.22	63	0.22 ± 0.03	0.98
C	0.43	63	0.30	1.0
D	0.87	63	0.73 ± 0.08	0.99
E	1.7	63	2.0 ± 0.9	N/A
F	0.43	15	0.4 ± 0.3	N/A
G	0.43	30	0.4 ± 0.2	N/A
H	0.43	130	0.55 ± 0.02	0.99
I	0.43	250	0.65 ± 0.1	0.97

* Coefficient of correlation for least-squares fits shown in Figures S5.1 and S5.2, where applicable.

Table S5.4: Least-squares analysis of log-transformed initial rates data from Table S5.3

Entry	Data fit (from Table S5.3)	Optimal model	r^2
A	A–E	$\log(v_0) = (-0.04 \pm 0.1) + (1.1 \pm 0.1) \cdot \log([\mathbf{1}]_0)$	0.98
B	C, F–I	$\log(v_0) = (-1.5 \pm 0.5) + (0.17 \pm 0.12) \cdot \log([H^+]_0)$	0.42

6. General Procedure for Time-resolved H_2 Quantification:

Inside of a nitrogen filled glovebox, the Fe precursor (**1** or **3**, 3.0 μmol) was added to a 500 mL round bottom flask as a solution in THF, and subsequently deposited as a thin film by removing the solvent in vacuo. To this flask was added solid $HBAr^F_4$ (0.44 mmol), KC_8 (0.56 mmol), and a stir bar. The flask was sealed with a septum at room temperature and subsequently chilled to -196 °C in the cold well of a nitrogen filled glovebox. Et_2O (7 mL) was added via syringe into the flask and completely frozen; the total volume of Et_2O was 7 mL, corresponding to a [Fe] = 0.43 mM and [$HBAr^F_4$] = 63 mM. The flask was passed out of the glovebox into a liquid N_2 bath, and subsequently thawed in a dry ice/acetone bath. The timer was set to zero as soon as the flask was transferred to the dry ice/acetone bath. The headspace of the reaction vessel was periodically sampled with a sealable gas sampling syringe (10 mL), which was immediately loaded into the GC, and analyzed for the presence of $H_{2(g)}$. From these data, the percent H_2 evolved (relative to $HBAr^F_4$) was calculated, correcting for the vapor pressure of Et_2O and the removed H_2 from previous samplings. Each time course was measured from a single reaction maintained at -78 °C. For the reaction using **1** as a precursor, the post-reaction material was analyzed for the presence of NH_3 via the methodology described above.

Table S6.1: Time profiles for the generation of H_2 in the presence of Fe precursors

Entry	Fe precursor	Time (min)	$H_{2(g)}$ (μmol)	% H_2 Based on H^+	% NH_3 Based on H^+
A	None	0	0	0	—
B		6	2.50	1.14	—
C		28	17.8	8.09	—
D		60	42.0	19.1	—
E		118	80.7	36.6	—
F		1039	169	76.7	—
G	**1**	0	0	0	—
H		5	8.63	3.92	—
I		25	53.5	24.3	—
J		45	72.4	32.9	—
K		66	74.0	33.6	—
L		118	78.2	35.5	—
M		1110	87.9	39.9	34
N	**3**	0	0	0	—
O		7.5	8.63	3.92	—
P		29	44.8	20.3	—
Q		60	133	60.6	—
R		119	190	86.0	—
S		945	195	88.4	—

7. Solution IR calibration of [Na(12-crown-4)$_2$][P$_3^B$Fe-N$_2$] (1):

A series of dilutions of **1** in THF were prepared, their solution IR spectra collected, and the absorbance at 1918 cm^{-1} (υ_{NN}) recorded (Table S7.1). A least-squares linear regression provides a calibration curve relating [**1**] (mM) to the absorbance of the N—N stretching mode (Fig. S7.1).

Table S7.1: Results of solution IR calibration of **1**

Entry	[1] (mM)	Abs @ 1918 cm^{-1} (a.u.)
A	1.25	0.3225
B	1.25	0.2495
Avg.	—	0.29 ± 0.05
A	2.5	0.5748
B	2.5	0.5295
Avg.	—	0.55 ± 0.03
A	5	1.0937
B	5	1.0471
Avg.	—	1.07 ± 0.03
A	10	1.7906
B	10	2.0769
Avg.	—	1.9 ± 0.2

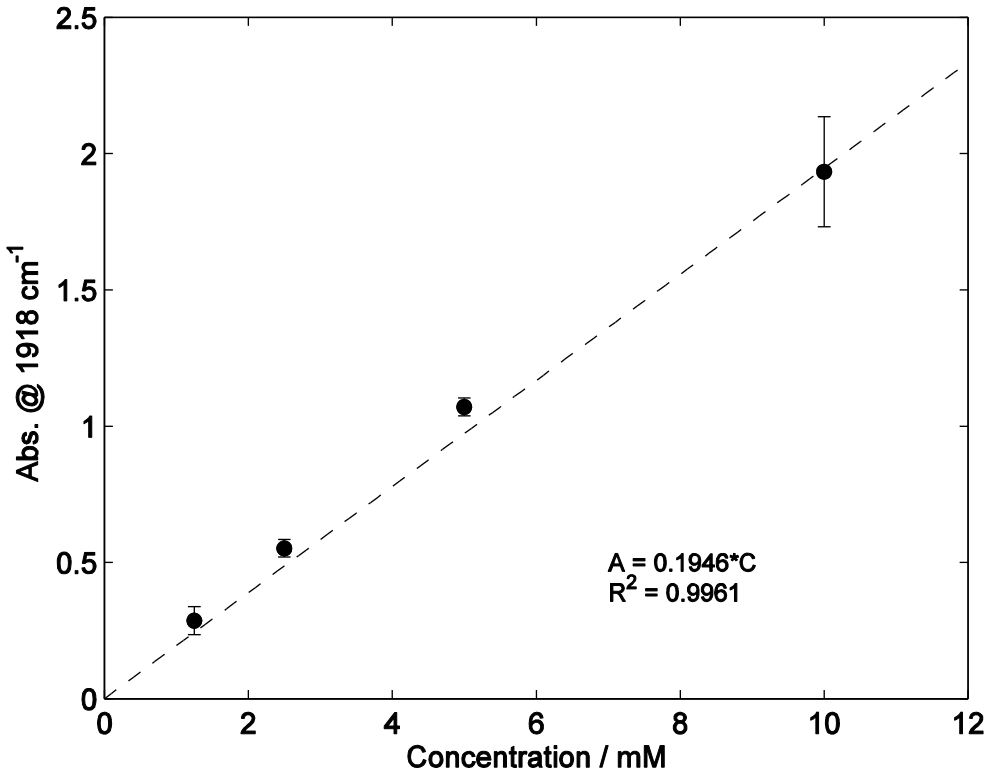

Figure S7.1: Solution IR calibration curve for **1**. Data for individual points are presented in Table S7.1

.

8. Stoichiometric reaction of $(P_3^B)(\mu\text{-}H)Fe(H)(N_2)$ (4-N_2) with $HBAr^F_4$ and KC_8:

Note that **4-N_2** is not indefinitely stable in the solid state, even at -30 °C; accordingly **4-N_2** was used within 24 hours after isolation as a solid

Reaction with $HBAr^F_4$ alone. To a solution of **4-N_2** (8 mg, 0.012 mmol) in 600 μL d_8-toluene was added a solution of $HBAr^F_4$ (12 mg, 0.012 mmol) in 100 μL Et_2O. This mixture was loaded into an NMR tube equipped with a J-Young valve and sealed. The tube was mixed over the course of 1.5 hrs with periodic monitoring by ^1H NMR (see Fig. S8.2). Over the course of this time the signals attributable to **4-N_2** slowly disappeared concomitant with the appearance of several new, paramagnetically-shifted resonances. An IR spectrum of the reaction material shows no characteristic resonances in the region from 1700–2500 cm^{-1} (except for a trace of residual **4-N_2** at 2070 cm^{-1}), suggesting the absence of terminally-coordinated N_2.

Sequential reaction with $HBAr^F_4$ and KC_8. A 20 mL scintillation vial was charged with a magnetic stir bar, **4-N_2** (5.0 mg, 0.0074 mmol), 0.75 mL of toluene and chilled to -78 °C in the cold well of a N_2 filled glove box. A solution of $HBAr^F_4$ (1.5 equiv, 11 mg, 0.011 mmol) was dissolved in 2.25 mL of Et_2O and similarly chilled. Subsequently, the ethereal $HBAr^F_4$ solution was added to the toluene solution of **4-N_2**, and the resultant mixture was stirred at low temperature for 1 hour, at which point it was pipetted into a pre-chilled vial containing solid KC_8 (6 equiv, 6.0 mg, 0.044 mmol). After stirring a low temperature for 30 minutes, this mixture was allowed to warm to room temperature for 15 minutes before all volatiles were removed in vacuo. The remaining solids were extracted with THF (2 x 1 mL) and filtered into a vial containing 6 μL of 12-crown-4. A sample of this filtrate was loaded into a solution IR cell and its spectrum was collected. The sharp resonance characteristic of **1** was observed at 1918 cm^{-1} (υ_{NN}), with an absorbance of 0.23, corresponding to [**1**] = 1.2 mM (0.0024 mmol, 32% yield, see Fig. S8.1). In addition to this resonance, a sharp resonance at 2070 cm^{-1} was observed, characteristic of **4-N_2** (υ_{NN}).

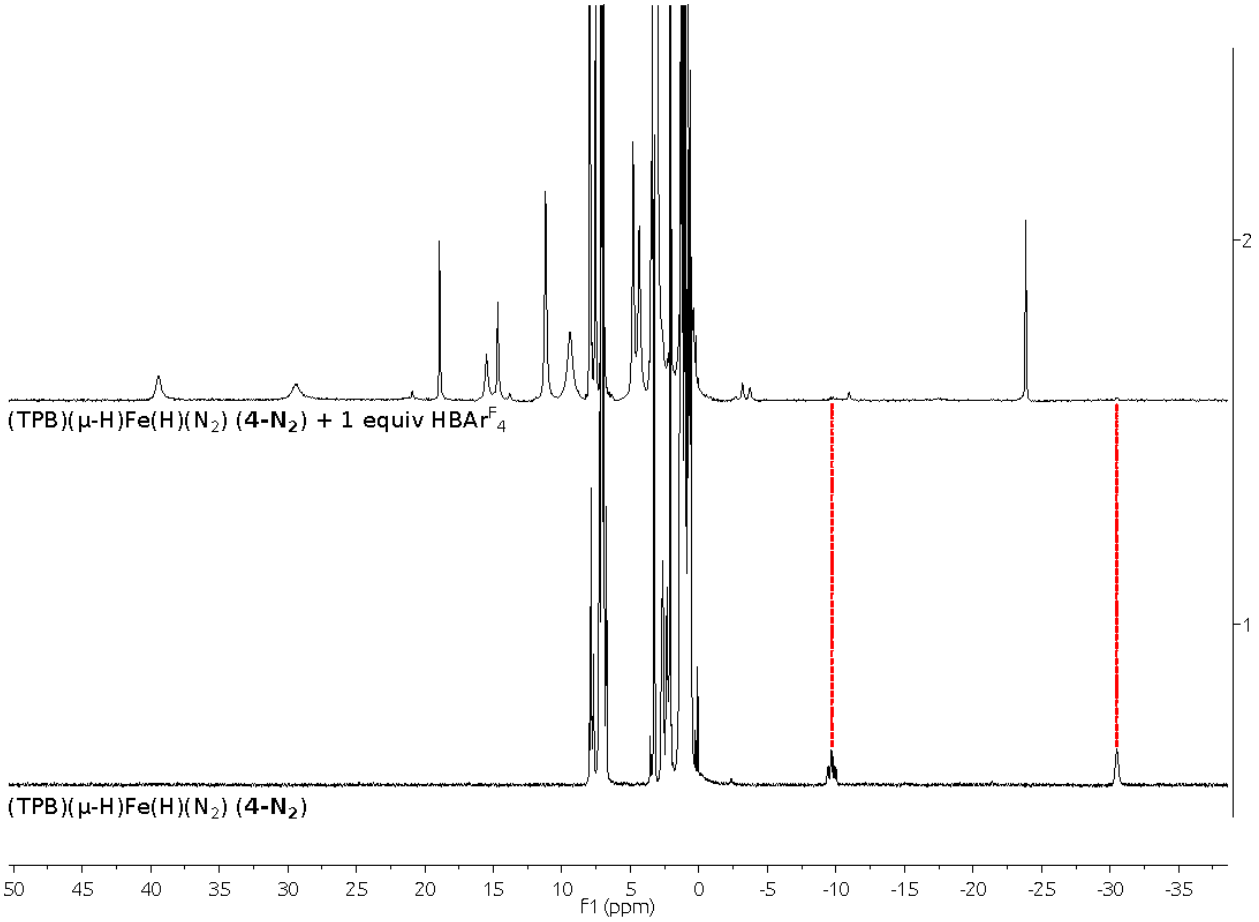

Figure S8.1: (Bottom) ^{1}H NMR spectrum of **4-N_2**, highlighting the characteristic hydride resonances appearing at ca. -10 and -30 ppm. (Top) Spectrum of the reaction between **4-N_2** and $HBAr^F_4$ in 6:1 d_8-toluene:Et_2O after 1.5 hrs of mixing at room temperature.

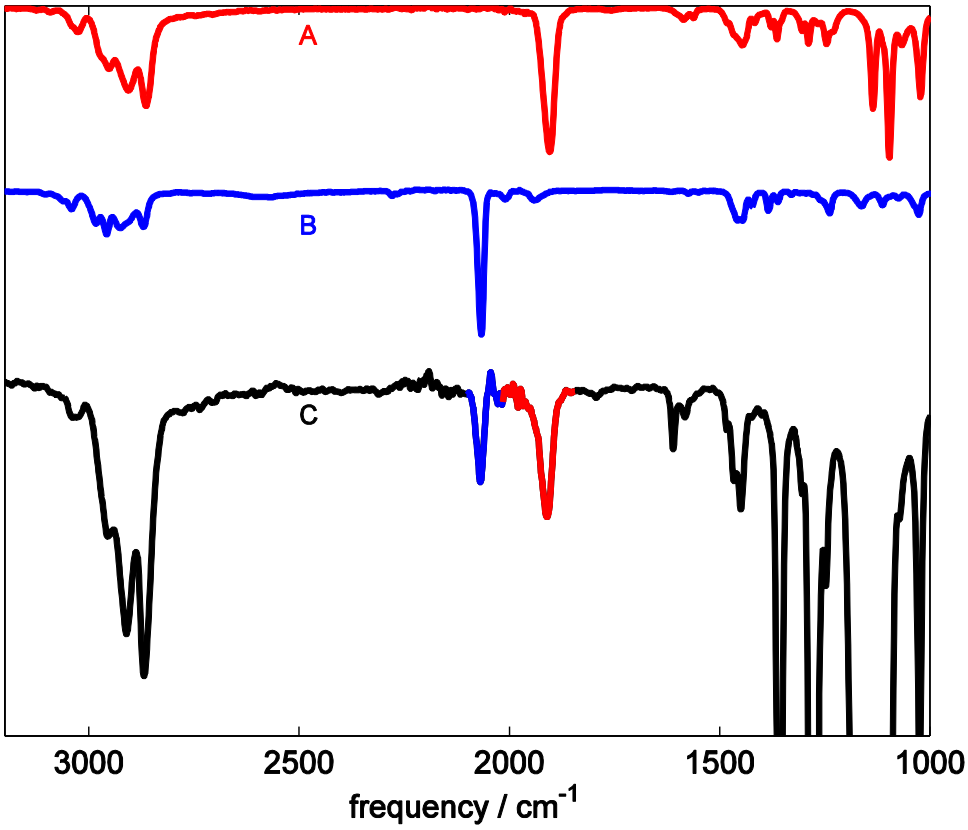

Figure S8.2: (A) Solid state IR spectrum of N_2 anion **1** deposited as a thin film from THF. (B) Solid state IR spectrum of hydride **4-N₂** deposited as a thin film from C_6D_6. (C) Solid state IR spectrum of the reaction mixture described in section 8 deposited as a thin film from THF.

9 Mössbauer Spectra:

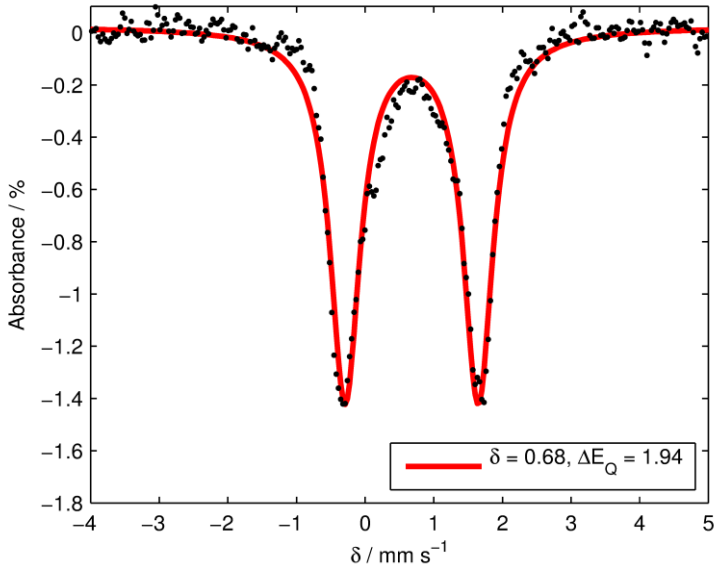

Figure S9.1: Zero field Mössbauer spectrum of $[P_3^BFe\text{-}NH_3][BAr^F{}_4]$, prepared by the addition of an atmosphere of $NH_{3(g)}$ to a solution of $[P_3^BFe][BAr^F{}_4]$ in 6:1 C_6D_6:THF. Raw data presented as black points, simulated data shown as a solid red line. Data collected on a frozen solution sample at 80 K.

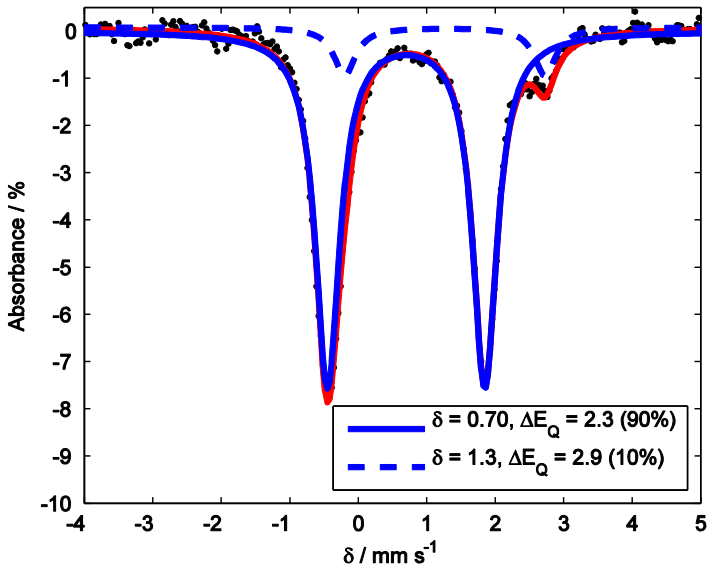

Figure S9.2: Zero field Mössbauer spectrum of $[P_3^BFe\text{-}N_2H_4][BAr^F{}_4]$, prepared by the addition of N_2H_4 to a solution of $[P_3^BFe][BAr^F{}_4]$ in 6:1 C_6D_6:THF. Raw data presented as black points, simulated data shown as a solid red line. The simulation is fit to two quadrupole doublets, that of $[P_3^BFe\text{-}N_2H_4][BAr^F{}_4]$ (solid blue line) and that of an unknown impurity (dashed blue line, < 10%). Data collected on a frozen solution sample at 80 K.

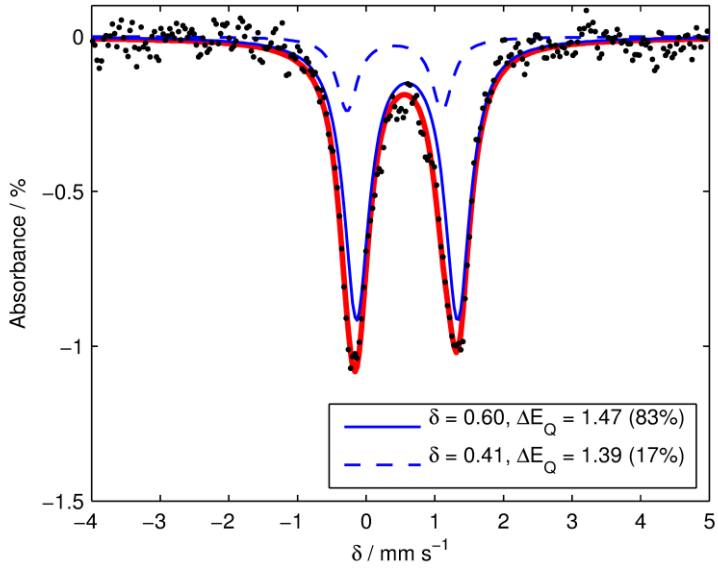

Figure S9.3: Zero field Mössbauer spectrum of $P_3^BFe\text{-}NH_2$, prepared by the addition $NaNH_2$ to a solution of $[P_3^BFe][BAr^F{}_4]$ in Et_2O. Raw data presented as black points, simulated data shown as a solid red line. The simulation is fit to two quadrupole doublets, that of $P_3^BFe\text{-}NH_2$ (solid blue line) and that of $P_3^BFe\text{-}OH$ (dashed blue line), resulting from NaOH contamination in $NaNH_2$. Data collected on a frozen solution sample at 80 K.

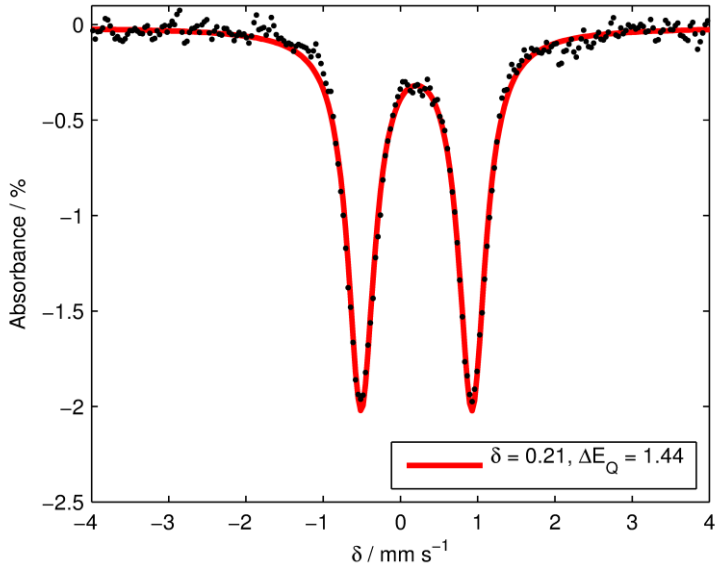

Figure S9.4: Zero field Mössbauer spectrum of $(P_3^B)(\mu\text{-}H)Fe(H)(N_2)$ (**4-N₂**), prepared by the addition of an H_2 atmosphere to a degassed solution of $P_3^BFe\text{-}N_2$ in C_6D_6, followed by removal of excess H_2 and mixing under an N_2 atmosphere overnight. Raw data presented as black points, simulated data shown as a solid red line. Data collected on a frozen solution sample at 80 K.

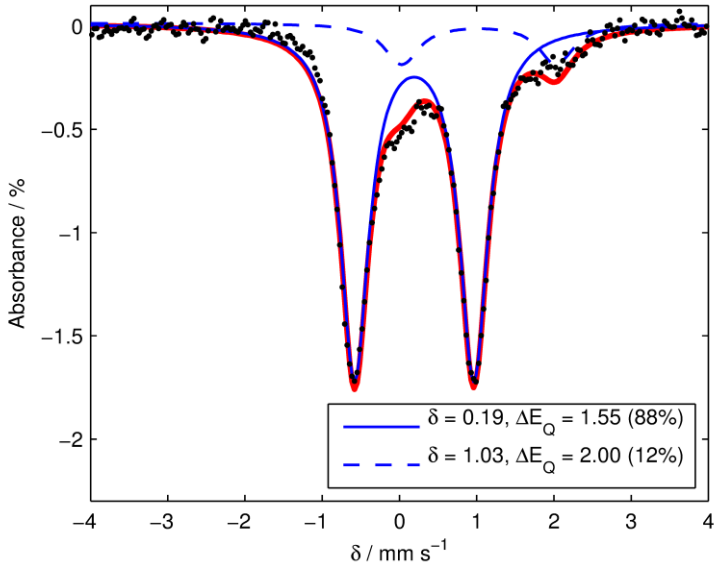

Figure S9.5: Zero field Mössbauer spectrum of (P_3^B)(μ-H)Fe(H)(H_2) (**4-H_2**), prepared by the addition of an H_2 atmosphere to a degassed solution of P_3^BFe-N_2 in C_6D_6. Raw data presented as black points, simulated data shown as a solid red line. The simulation is fit to two quadrupole doublets, that of **4-H_2** (solid blue line) and that of unknown decomposition product(s) (dashed blue line), likely resulting from B–C bond cleavage under excess H_2. Data collected on a frozen solution sample at 80 K.

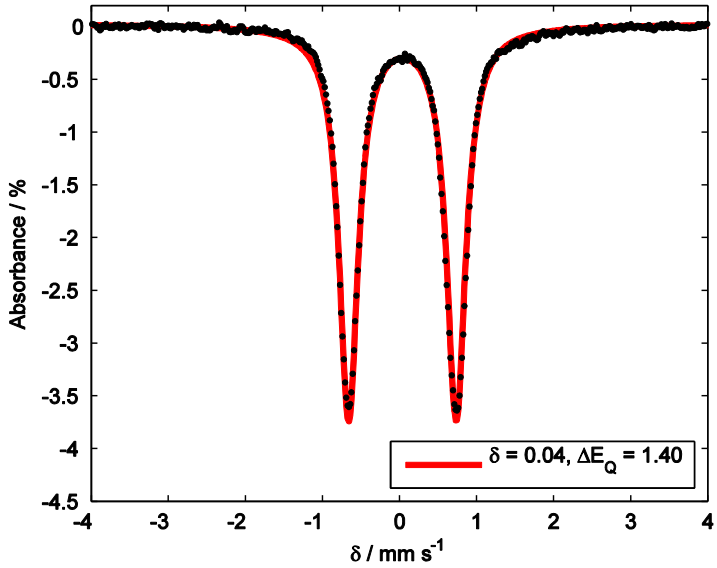

Figure S9.6: Zero field Mössbauer spectrum of P_3^BFe-NAd. Raw data presented as black points, simulated data shown as a solid red line. Data collected on a powder sample at 80 K.

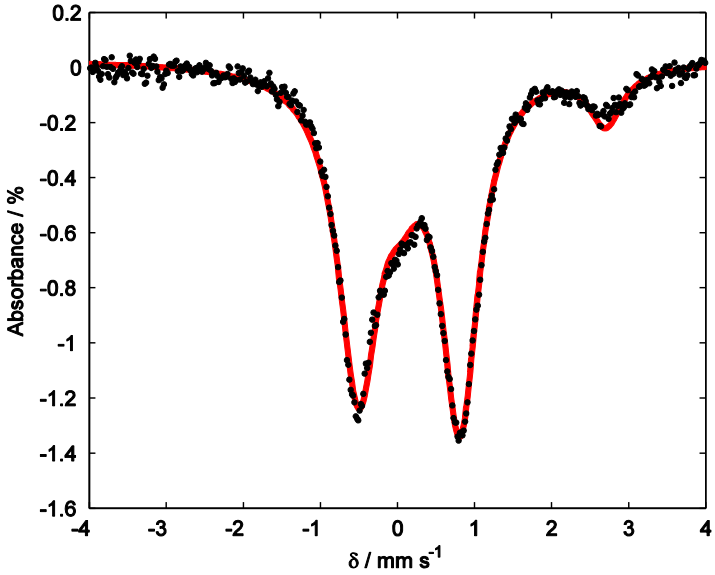

Figure S9.7: Zero field Mössbauer spectrum of [P_3^BFe-NAd][BAr^F_4]. Raw data presented as black points, simulated data shown as a solid red line. The simulation is fit to two quadrupole doublets, that of [P_3^BFe-NAd][BAr^F_4] (90%) and that of unknown high spin decomposition product (~10%). Data collected on a powder sample at 80 K in the presence of a 50 mT external magnetic field (parallel mode).

10. Rapid-freeze-quench Mössbauer

10.1 General Procedure for Preparation of Rapid-freeze-quench Mossbauer Samples of Catalytic Reaction Mixtures using 1:

All manipulations are carried out inside of a nitrogen filled glovebox. Into a 150 mL Schlenk tube (51 mm OD) is deposited a film of $[Na(12\text{-crown-}4)_2][P_3{}^{B\,57}Fe\text{-}N_2]$ from a freshly prepared stock solution in THF. The tube is charged with a 25 mm stir bar and chilled to -196 °C in dewar filled with liquid N_2. A solution of $HBAr^F{}_4$ in Et_2O is added to the chilled tube and allowed to freeze; subsequently a suspension of KC_8 in Et_2O is added and also allowed to freeze. The tube is sealed, and transferred to a pre-chilled cold well at -78 °C (the cold well temperature is monitored directly with a thermocouple). The timer is set to zero as soon as the stir bar is freed from the thawing solvent. At the desired time, the tube is opened, and ~1 mL of the well-stirred suspension is transferred to a Delrin cup pre-chilled to -78 °C using a similarly pre-chilled pipette. The sample in the Delrin cup is then rapidly frozen in liquid N_2. At this point the sample, immersed in liquid N_2, is taken outside of the glovebox and mounted in the cryostat.

10.2 General Procedure for Fitting of Rapid-freeze-quench Mössbauer Samples:

Data analysis was performed using version 4 of the program WMOSS (www.wmoss.org) and quadrupole doublets were fit to Lorentzian lineshapes. Simulations were constructed from the minimum number of quadrupole doublets required to attain a quality fit to the data (convergence of $\chi_R{}^2$). Quadrupole doublets were constrained to be symmetric, unless **1** was included in the model (the presence of **1** in samples was confirmed by comparison of zero-field spectra with spectra collected in an external 50 mT magnetic field, which dramatically sharpens the resonances attributable to **1**; see ref. 7). Using the non-linear error analysis algorithm provided by WMOSS, the errors in the computed parameters are estimated to be 0.02 mm s^{-1} for δ and 2% for ΔE_Q.

10.3. Details of Individual RFQ Mossbauer spectra:

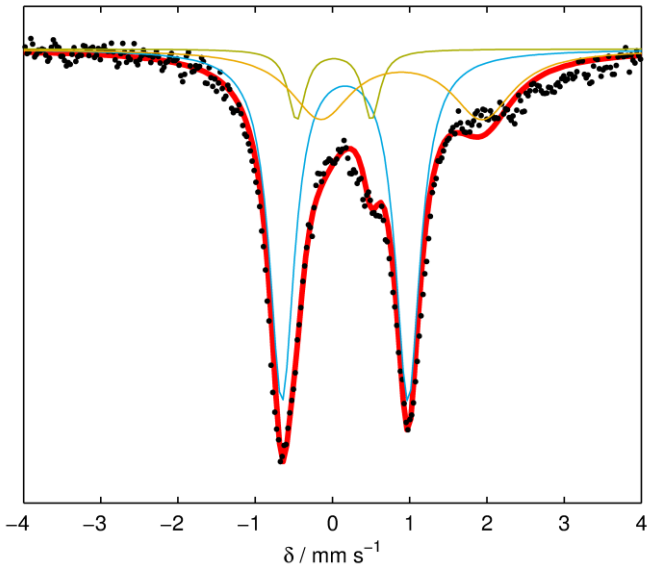

Figure S10.1: Mossbauer spectrum collected from a catalytic reaction quenched after 5 minutes. Conditions: [[Na(12-crown-4)$_2$][P_3^B ^{57}Fe-N_2]] = 0.64 mM, [[H(OEt$_2$)$_2$][Bar$^F_4$]] = 31 mM (48 equiv), 1.2 equiv KC_8 relative to [H(OEt$_2$)$_2$][Bar$^F_4$]. Raw data shown as black points, simulation as a solid red line, with components in blue, green, orange (see Table S10.1 for parameters). Collected at 80 K with a parallel applied magnetic field of 50 mT.

Fitting details for Figure S10.1: Three pairs of quadrupole doublets were found to be necessary to obtain an adequate simulation of these data. The simulation parameters are given in Table S10.1. The major component (shown in blue in Fig. S10.1) is the only species with resolved lineshapes, while the remaining components (shown in green and orange) were fit to the broad residual signal by least-squares refinement. While this fitting procedure is necessary to get an accurate integration of the major species, the Mossbauer parameters for the minor components should not be considered reliable. It is possible that the broad residual signal arises from multiple minor components whose resonances are not well-resolved.

Table S10.1: Simulation parameters for Mossbauer spectrum in Figure S10.1

Component	δ (mm s^{-1})	ΔE_Q (mm s^{-1})	Linewidths, Γ_L/ Γ_R (mm s^{-1})	Relative area
A (blue)	0.16 ± 0.02	1.63 ± 0.03	0.39/0.39	0.61
B (green)	0.02 ± 0.02	0.97 ± 0.02	0.27/0.27	0.085
C (orange)	0.89 ± 0.02	2.10 ± 0.04	0.96/0.96	0.28

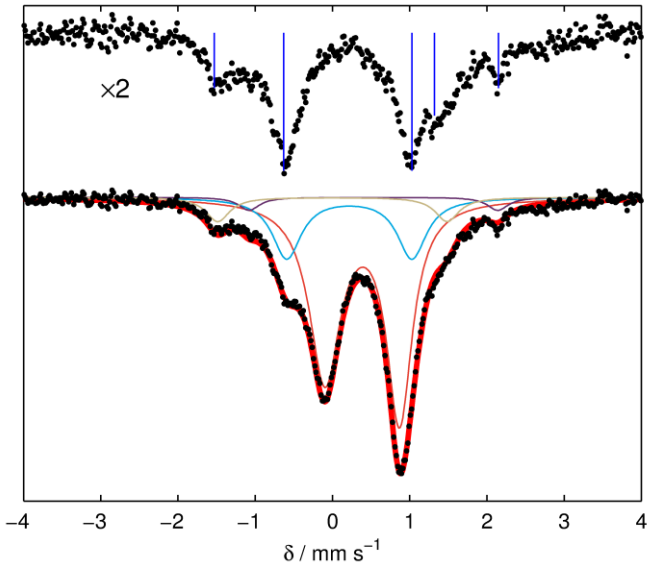

Figure S10.2: Mossbauer spectrum collected from a catalytic reaction quenched after 25 minutes. Conditions: [[Na(12-crown-4)$_2$][$P_3^{B\,57}$Fe-N_2]] = 0.64 mM, [[H(OEt$_2$)$_2$][Bar$^F_4$]] = 31 mM (48 equiv), 1.2 equiv KC_8 relative to [H(OEt$_2$)$_2$][Bar$^F_4$]. (Bottom) Raw data shown as black points, simulation as a solid red line, with components in blue, red, tan, and purple (see Table S10.2 for parameters). (Top) Raw data after subtraction of major component, shown at twice the scale of the bottom spectrum for clarity. Collected at 80 K with a parallel applied magnetic field of 50 mT.

Fitting details for Figure S10.2: Four quadrupole doublets were found to be necessary to obtain an adequate simulation. The simulation parameters are given in Table S10.2. The major species present in this spectrum is well-simulated by the parameters of **1**. After subtraction of this component, the residual signal exhibits five resolved lines, indicating the presence of at least three quadrupole doublets (Fig. S10.2, Top). The most intense of these has parameters nearly identical to species A in Table S10.1. The remaining signal is well-simulated by two sharp quadrupole doublets, one with parameters nearly identical to those of P_3^BFe-N_2 (D, purple), and one novel species with an unusually low isomer shift (C, tan).

Table S10.2: Simulation parameters for Mossbauer spectrum in Figure S10.2

Component	δ (mm s^{-1})	ΔE_Q (mm s^{-1})	Linewidths, Γ_L/ Γ_R (mm s^{-1})	Relative area
A (blue)	0.22 ± 0.02	1.62 ± 0.03	0.46/0.46	0.22
B (red)	0.39 ± 0.02	0.97 ± 0.02	0.49/0.40	0.70
C (tan)	0.00 ± 0.02	2.97 ± 0.06	0.37/0.37	0.072
D (purple)	0.53 ± 0.02	3.22 ± 0.06	0.33/0.33	0.034

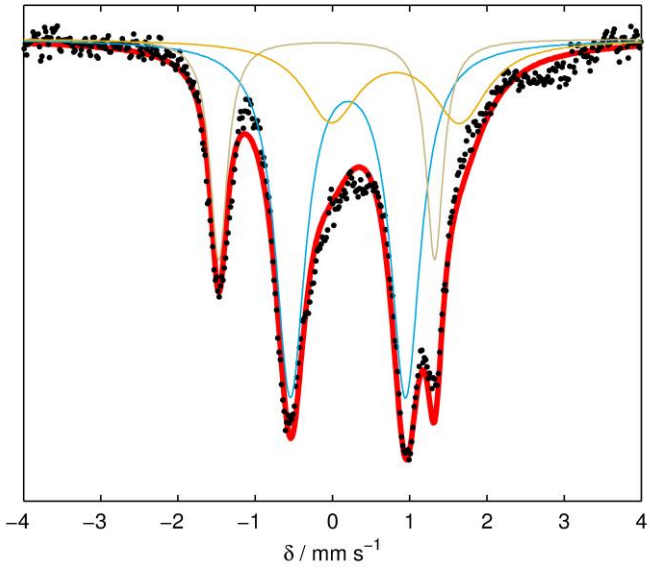

Figure S10.3: Mossbauer spectrum collected from a catalytic reaction quenched after 5 minutes. Conditions: [[Na(12-crown-4)$_2$][$P_3^{B\,57}$Fe-N_2]] = 0.43 mM, [[H(OEt$_2$)$_2$][Bar$^F_4$]] = 63 mM (150 equiv), 1.2 equiv KC_8 relative to [H(OEt$_2$)$_2$][Bar$^F_4$]. Raw data shown as black points, simulation as a solid red line, with components in blue, tan, and orange (see Table S10.3 for parameters). Collected at 80 K with a parallel applied magnetic field of 50 mT.

Fitting details for Figure S10.3: Four quadrupole doublets were found to be necessary to obtain an adequate simulation. The simulation parameters are given in Table S10.3. The major species present in this spectrum has parameters very similar to those of the major component in the spectrum in Figure S10.1 (Table S10.1, A); indeed, in both cases this species comprises approximately 60% of the signal. This spectrum also features a second well-resolved quadrupole doublet, which has parameters nearly identical to those of the novel minor component shown in tan in Figure S10.2 (Table S10.2, C). As with the spectrum in Figure S10.1, after fitting these two resolved doublets there is a broad residual signal centered around 0.8 mm s^{-1}. Due to the broadness of this signal, the parameters for this component should not be considered reliable, but its inclusion in the simulation is required for accurate integration.

Table S10.3: Simulation parameters for Mossbauer spectrum in Figure S10.3

Component	δ (mm s^{-1})	ΔE_Q (mm s^{-1})	Linewidths, Γ_L/ Γ_R (mm s^{-1})	Relative area
A (blue)	0.20 ± 0.02	1.49 ± 0.03	0.47/0.47	0.61
B (tan)	-0.07 ± 0.02	2.80 ± 0.06	0.27/0.27	0.23
C (orange)	0.82 ± 0.02	1.67 ± 0.03	0.87/0.87	0.25

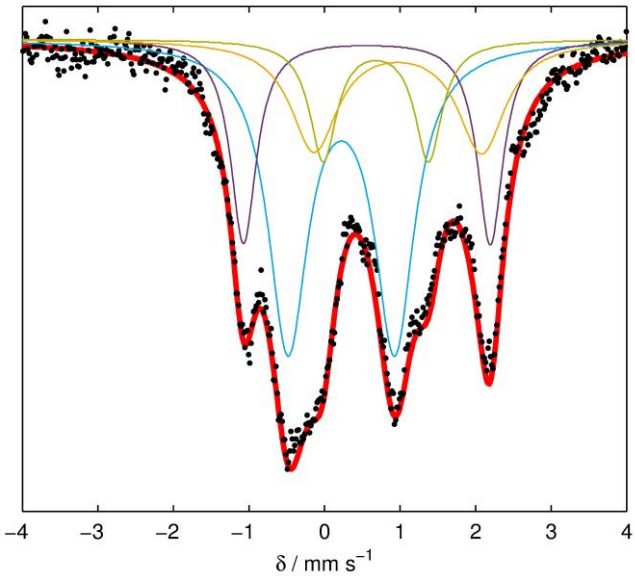

Figure S10.4: Mossbauer spectrum collected from a catalytic reaction quenched after 10 minutes. Conditions: [[Na(12-crown-4)$_2$][$P_3^{B\,57}$Fe-N_2]] = 0.43 mM, [[H(OEt$_2$)$_2$][Bar$^F_4$]] = 63 mM (150 equiv), 1.2 equiv KC_8 relative to [H(OEt$_2$)$_2$][Bar$^F_4$]. Raw data shown as black points, simulation as a solid red line, with components in blue, purple, green, and orange (see Table S10.4 for parameters). Collected at 80 K with a parallel applied magnetic field of 50 mT.

Fitting details for Figure S10.4: Four quadrupole doublets were found to be necessary to obtain an adequate simulation. The simulation parameters are given in Table S10.4. The spectrum shown in Figure S10.4 exhibits six clearly resolved features, indicating at least three pairs of quadrupole doublets. The two most extreme resonances are well-modeled by the parameters for P_3^BFe-N_2. After fitting this component (purple), the residual signal shows a pair of nearly overlapping quadrupole doublets, as well as an additional broad baseline component centered around 1 mm s^{-1}. The resolved features fit to two species, one with parameters nearly identical to those of the major species show in Figure S10.3 (Table S10.3, A), and another with parameters quite similar to those of P_3^BFe-NH_2 (green). As with previous spectra, a final component (orange) was included to model the broad residual baseline signal.

Table S10.4: Simulation parameters for Mossbauer spectrum in Figure S10.4

Component	δ (mm s^{-1})	ΔE_Q (mm s^{-1})	Linewidths, Γ_L/ Γ_R (mm s^{-1})	Relative area
A (blue)	0.22 ± 0.02	1.41 ± 0.03	0.64/0.64	0.50
B (purple)	0.56 ± 0.02	3.27 ± 0.07	0.41/0.41	0.22
C (green)	0.68 ± 0.02	1.40 ± 0.03	0.44/0.44	0.14
D (orange)	0.97 ± 0.02	2.22 ± 0.04	0.76/0.76	0.21

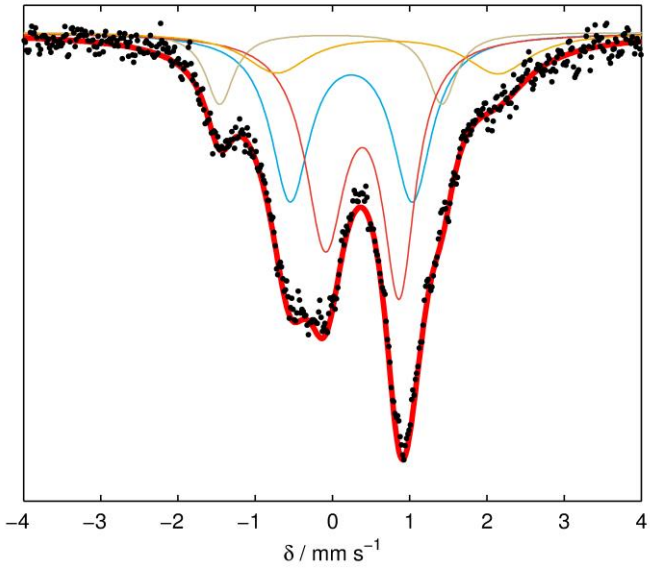

Figure S10.5: Mossbauer spectrum collected from a catalytic reaction quenched after 25 minutes. Conditions: [[Na(12-crown-4)$_2$][$P_3^{B\,57}$Fe-N_2]] = 0.43 mM, [[H(OEt$_2$)$_2$][Bar$^F_4$]] = 63 mM (150 equiv), 1.2 equiv KC_8 relative to [H(OEt$_2$)$_2$][Bar$^F_4$]. Raw data shown as black points, simulation as a solid red line, with components in blue, purple, green, and orange (see Table S10.5 for parameters). Collected at 80 K with a parallel applied magnetic field of 50 mT.

Fitting details for Figure S10.5: Four quadrupole doublets were found to be necessary to obtain an adequate simulation. The simulation parameters are given in Table S10.5. The spectrum shown in Figure S10.5 exhibits four clearly resolved features, the intensities of which indicate at least three pairs of quadrupole doublets. The major component is well modeled by the parameters for **1** (red). After subtraction of this component, the residual signal exhibits two resolved quadrupole doublets in addition to a broad baseline signal centered around 0.7 mm s^{-1}. The two resolved species fit well to the two major components shown in Figure S10.3 (blue and tan), while the residual signal was fit to a broad quadrupole doublet for accurate integration.

Table S10.5: Simulation parameters for Mossbauer spectrum in Figure S10.5

Component	δ (mm s^{-1})	ΔE_Q (mm s^{-1})	Linewidths, Γ_L/ Γ_R (mm s^{-1})	Relative area
A (blue)	0.24 ± 0.02	1.58 ± 0.03	0.61/0.61	0.39
B (red)	0.39 ± 0.02	0.96 ± 0.02	0.63/0.51	0.49
C (tan)	-0.02 ± 0.02	2.88 ± 0.06	0.44/0.44	0.13
D (orange)	0.71 ± 0.02	2.87 ± 0.06	1.01/1.01	0.15

N.B. Note that the simulations of each of the spectra above were allowed to refine freely by a least-squares optimization model. Given that each spectrum reflects a mixture of species, some uncertainty in the fitting parameters is expected. Operating under the assumption that the signal assigned to species A in Tables S10.1–S10.5 is due to the same Fe compound, then we can estimate the uncertainty in the spectral simulations by the standard deviation in the optimized fits for each spectrum. We thus assign the parameters of A as δ = 0.21 ± 0.03 mm s^{-1} and ΔE_Q = 1.55 ± 0.09 mm s^{-1}. Performing the same analysis for the tan components in Tables S10.2, S10.3, and S10.5 yields parameters δ = -0.03 ± 0.04 mm s^{-1} and ΔE_Q = 2.88 ± 0.09 mm s^{-1}.

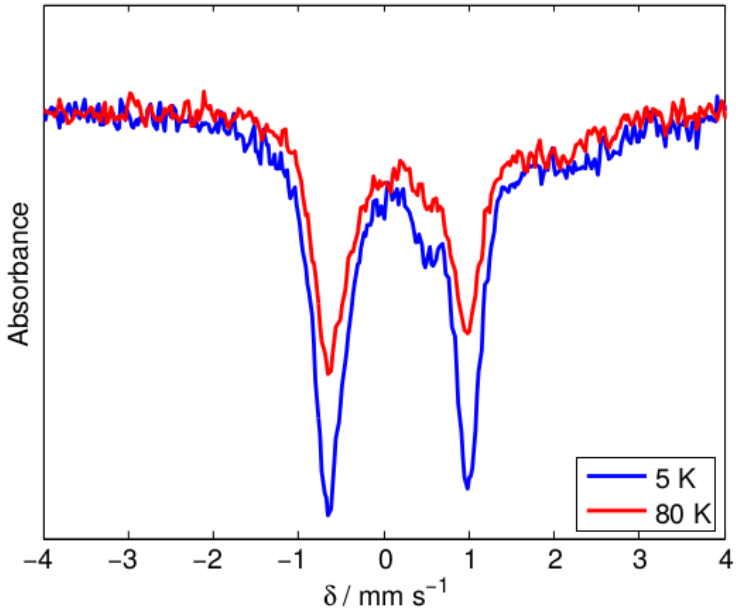

Figure S10.6: Low temperature Mossbauer spectrum of freeze-quenched catalytic reaction mixture. The sample is identical to that presented in Figure S10.1. Data collected in a 50 mT parallel magnetic field at 80 K (red trace) and 5 K (blue trace). The lack of magnetic hyperfine interactions in the 5 K spectrum of the major component strongly favors a non-Kramers spin system assignment.

11. Controlled Potential Electrolysis of $[P_3^BFe][BAr^F_4]$ and $HBAr^F_4$

General considerations. All manipulations were carried out in an N_2 filled glove box. A sealable H-cell consisting of two compartments separated by a fine porosity sintered glass frit was charged with 15 mL (working chamber) and 7 mL (auxiliary chamber) of 0.1 M Na BAr^F_4 solution in Et_2O. The working chamber was outfitted with a reticulated vitreous carbon working electrode (100 pores per inch (ppi) grade obtained from K.R. Reynolds Company, prepared by holding the electrode at -3.0 V vs Fc/Fc^+ in a separate 0.1 M $NaBAr^F_4$ solution for 30 minutes and rinsing with Et_2O), the working electrode was rectangular prismatic in shape with dimensions of 10 mm x 6 mm and was submerged in the working chamber solution to a depth of ~2-3 mm. The working chamber also featured a $Ag/AgPF_6$ in Et_2O reference electrode isolated by a CoralPor™ frit (obtained from BASi) and referenced externally to Fc/Fc^+. The auxiliary chamber was outfitted with a Zn foil electrode of dimensions 21.5 cm x 1.5 cm. The cell was cooled to -45 °C in a cold well and then sealed before electrolysis. The cell was connected to a CH Instruments 600B electrochemical analyzer and controlled potential bulk electrolysis experiments were performed at -45 °C with stirring.

Electrolysis with 10 equiv $HBAr^F_4$ at -2.6 V vs Fc/Fc^+. To the working chamber was added 11.3 mg of $[P_3^BFe][BAr^F_4]$ (7.5 μmol), 76 mg of $HBAr^F_4$ (75 μmol), and a magnetic stir bar. The cell passed 5.85 C of charge over the course of 4.6 hours. After that time the potential bias was removed, the headspace of the cell was sampled with a sealable gas syringe (10 mL), which was immediately analyzed by GC for the presence of $H_{2(g)}$. Then $HBAr^F_4$ solutions in Et_2O were injected through rubber septa into both chambers to sequester NH_3 as $[NH_4][BAr^F_4]$ (25 mg, 25 μmol for the working chamber and 10 mg, 10 μmol for the auxiliary chamber). The cell was allowed to stir at -45 °C for 10 minutes and then warmed to room temperature and stirred an additional 15 minutes. The contents of both chambers were then transferred to a Schlenk tube (cell washed with additional Et_2O) and this material was analyzed for NH_3 by base digestion, vacuum transfer of volatiles, and the indophenol method as described in section 1.4. The results of the two product analyses were that 3.5 μmol of NH_3 and 17.5 μmol of H_2 had been produced.

Electrolysis with 50 equiv $HBAr^F_4$ at -2.3 V vs Fc/Fc^+. To the working chamber was added 5.0 mg of $[P_3^BFe][BAr^F_4]$ (3.3 μmol), 170 mg of $HBAr^F_4$ (168 μmol), and a magnetic stir bar. The cell passed 8.39 C of charge over the course of 16.5 hours. After that time the potential bias was removed, the headspace of the cell was sampled with a sealable gas syringe (10 mL), which was immediately analyzed by GC for the presence of $H_{2(g)}$, and $HBAr^F_4$ solutions in Et_2O were injected through rubber septa into both chambers to sequester NH_3 as $[NH_4][BAr^F_4]$ (40 mg, 40 μmol for the working chamber and 20 mg, 20 μmol for the auxiliary chamber). The cell was allowed to stir at -45 °C for 10 minutes and then warmed to room temperature and stirred an additional 15 minutes. The contents of both chambers were then transferred to a Schlenk tube (cell washed with additional Et_2O) and this material was analyzed for NH_3 by base digestion, vacuum transfer of volatiles, and the indophenol method as described in section 1.4. The results of the two product analyses were that 7.3 μmol of NH_3 and 21.7 μmol of H_2 had been produced.

References:

[1] Wietz, I. S.; Rabinovitz, M. J. *J. Chem. Soc., Perkin Trans.* **1993**, *1*, 117.
[2] Moret, M.-E.; Peters, J. C. *Angew. Chem. Int. Ed.* **2011**, *50*, 2063.
[3] Creutz, S. E.; Peters, J. C. *J. Am. Chem. Soc.* **2014**, *136*, 1105.
[4] Mankad, N. P.; Whited, M. T.; Peters, J. C. *Angew. Chem. Int. Ed.* **2007**, *46*, 5768.

[5] Fong, H.; Moret, M.-E.; Lee, Y.; Peters, J. C. *Organometallics* **2013**, *32*, 3053.
[6] Anderson, J. S.; Moret, M.-E.; Peters, J. C. *J. Am. Chem. Soc.* **2012**, *135*, 534.
[7] Anderson, J. S.; Cutsail, G. E. III; Rittle, J.; Connor, B. A.; Gunderson, W. A.; Zhang, L.; Hoffman, B. M.; Peters, J. C. *J. Am. Chem. Soc.* **2015**, *137*, 7803.
[8] Weatherburn, M. W. *Anal. Chem.* **1967**, *39*, 971.
[9] Reger, D. L.; Little, C. A.; Lamba, J. J. S.; Brown, K. J.; Krumper, J. R.; Bergman, R. G.; Irwin, M.; Fackler Jr., J. P. *Inorg. Synth.* **2004**, *34*, 5.
[10] Yakelis, N. A.; Bergman, R. G. *Organometallics* **2005**, *24*, 3579.
[11] Brookhart, M.; Grant, B.; Volpe Jr., A. F. *Organometallics* **1992**, *11*, 3920.
[12] Watt, G. W.; Chrisp, J. D. *Anal. Chem.* **1952**, *24*, 2006.
[13] Anderson, J. S.; Rittle, J.; Peters, J. C. *Nature* **2013**, *501*, 84.